arXiv:nlin/0204047v1 [nlin.AO] 18 Apr 2002

FRACTAL EVOLUTION OF NORMALIZED FEEDBACK SYSTEMS ON A LATTICE

Siegfried Fussy
Gerhard Grössing

Austrian Institute for Nonlinear Studies,
Parkgasse 9, A-1030 Vienna, Austria
http://web.telekabel.at/ains

Abstract

Highly nonlinear behaviour of a system of discrete sites on a lattice is observed when a specific feedback loop is introduced into models employing quantum cellular automata [1] or their real-valued analogues.

It is shown that the combination of two operations, i.e. i) enhancement of a site's value when fulfilling a feedback condition and ii) normalization of the system after each time step, produces relatively short-lived spatiotemporal patterns whose mean lifetime can be considered as emergent order parameter of the system. This mean lifetime obeys a scaling law involving a control parameter which tunes the "fault tolerance" of the feedback condition. Thus, within appropriate ranges of the systems variables, the dynamical properties can be characterized by a "fractal evolution dimension" (as opposed to a "fractal dimension").

1 Introduction

The study of spatiotemporal patterns in dynamical systems has brought some general insights into the mechanisms of pattern generation and evolution. Applications exist not only for physical or chemical systems exhibiting chaotic behaviour [2] but also for models of biological networks [3].

Above all, it has turned out that the systems descriptions via discrete maps help to avoid complications arising from the analysis of integro-differential equations [4, 5]. One important tool for model building is the use of coupled-map lattices, either with global couplings as in [6], i.e.

$$x(t+1,j) = (1-\zeta)\, f(x(t,j)) + \frac{\zeta}{N} \sum_{i=1}^{N} f(x(t,i))\,, \qquad j = 1,\ldots,N\,, \quad (1)$$

where t denotes a discrete time step, j the index of elements of a one-dimensional array and ζ the coupling constant, or with local couplings permitting only nearest-neighbour interaction [7], i.e.

$$x(t+1,j) = (1-\zeta)\, f(x(t,j)) + \frac{\zeta}{2}\{f(x(t,j-1)) + f(x(t,j+1))\} \qquad j = 1,\ldots,N\,. \tag{2}$$

The mapping function $f(x)$ is usually chosen as nonlinear function, e.g. $f(x) = 1 - ax^2$. Thus the systems dynamics is governed by a diffusing part (tuned by ζ) and a nonlinear transformation (tuned by a).

Another approach consists of the simulation of the systems' evolutions by cellular automata [8], where time, space and the values of the state variables (sites) are discrete. As opposed to the coupled-map models, the source of complexity is the large number of degrees of freedom and not a nonlinear map.

In this paper we choose a different approach to complex pattern formation: we first consider the quantum mechanical analogue of Eq. (2), but with a linear mapping function. For the sake of probability conservation, a normalization procedure after each time step has to be introduced, which on one hand represents a source of nonlinearity. On the other hand, it implies a kind of nonlocal information spreading all over the array, similar to the global coupling in (1). This model was introduced as quantum cellular automaton (QCA) some years ago and it was also applied as discretized version of the Schrödinger equation [9].

In its most elementary form the evolution rule reads as

$$\Psi(t,j) = \frac{1}{\sqrt{\mathcal{N}(t)}}\{\Psi(t-1,j) + i\delta\Psi(t-1,j-1) + i\delta^*\Psi(t-1,j+1)\}\,, \quad \Psi,\delta \in \mathcal{C} \tag{3}$$

with δ as coupling constant and $\mathcal{N}$ as normalization factor yielding

$$\begin{array}{c} \rho(t,j) := |\Psi(t,j)|^2\,, \\ \sum_{j=1}^{N} \rho(t,j) = 1 \qquad \text{for all } t\,. \end{array} \tag{4}$$

The normalized values $\rho(t,j)$ can be interpreted as probability densities for the chosen one-dimensional arrays and are used furtheron for presentation of the results. This system has been studied thoroughly [10]. It exhibits the emergence of exactly predictable coherent large-scale patterns. In fact, the effect of the nonlinearity introduced by normalization is not strong enough to prevent an exact long-term prediction of its evolution.

Therefore, to increase the complexity, we provide the system with a memory in which the sites' values of the last few hundred time steps are stored. If a specific feedback condition applied to each site is fulfilled for any site, the value of that particular site is enhanced. Then the array has to be normalized again. Thus the necessary conservation of probability is guaranteed by confining all possible (continuous) values of the sites within the domain $[0,1]$. Consequently, the arising patterns built by a group of nonvanishing sites in the spatiotemporal plane can be compared with each other, both when $|\delta| << 1$ and $|\delta| >> 1$.

In the following, we shall focus on only one specific temporal feedback operation [11]. It will be shown that the complexity of the systems' behaviours increases considerably due to this second source of nonlinearity. We think that the arising features of self-organization can serve as canditates to understand, at least in principle, some aspects of neural activity, particulary in those domains where quantum theory would be necesssary to model neural interactions [12].

2 Fractal evolution

For the purpose of illustration, but without loss of generality, we choose the parameters of our model as follows. The systems variables for the "undisturbed" one-dimensional QCA (cf. Eq. (3)) are the size N (i.e. the number of sites), the initial values of the state variables $\Psi(0,j)$, and the mixing parameter $\delta = |\delta|e^{i\phi}$, $\phi \in \mathcal{R}$. They are chosen as

$$\begin{gathered} N = 120 \\ \Psi(0,40) = 0.1\,, \quad \Psi(0,60) = 0.9\,, \quad \Psi(0,100) = 0.3 \\ \delta \equiv \delta_c \cdot (1+i) = 0.02(1+i)\,. \end{gathered} \tag{5}$$

The single feedback operation acts on the time coordinate, such that a kind of memory is introduced into the system. This operation becomes effective after t_{mem} time steps. Accordingly, the memory of the system consists of an array of the size $t_{mem} \times N$ where the sites' values are stored and cyclically shifted after each time step to keep the most recent values of the array. After having reached t_{mem}, at each time step $t > t_{mem}$ it is checked whether the normalized absolute value of each site of the array is similar to its value at the time $t - t_{mem}$. The similarity check is done by asking whether the present value lies within a specific range of the past value. A "relative interval width" ϵ is introduced as crucial control parameter of the model:

$$\left|\left|\frac{\Psi(t,j)}{\Psi(t-t_{mem},j)}\right| - 1\right| < \epsilon \quad \text{for all } j, \text{ and } t > t_{mem} \tag{6}$$

where ϵ varies between 0.0 $(= 0\%)$ and 1.0 $(= 100\%)$.

If the condition (6) is fulfilled, the value of the site under consideration is amplified by setting it to $A_{amp} >> 1$

$$\Psi(t,j)_{enhanced} = A_{amp}\,. \tag{7}$$

Thereafter, the usual normalization procedure is applied.

Note that this kind of feedback operation simulates a selection process enhancing the values and, consequently, the further evolutions of those sites which fulfill the similarity condition. We expect that because of the simplicity of the basic model and the additional feedback operation some features of simple neuronal systems could be modelled, at least with respect to their principal dynamical structures (cf. [12]).

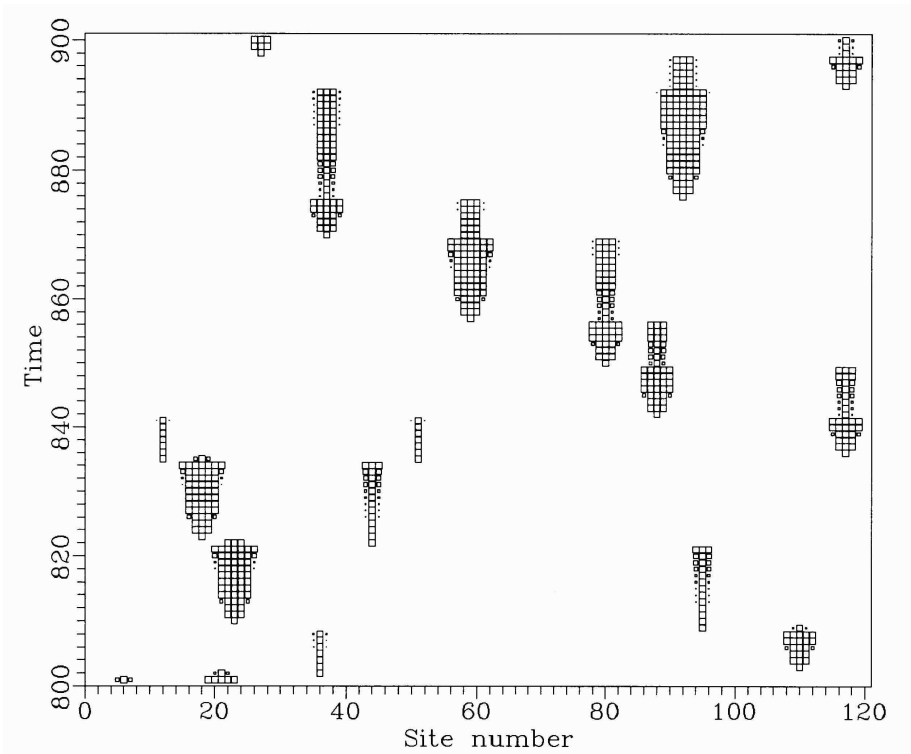

Figure 1: Density plot of a QCA with temporal feedback loop accentuating the range of the box values from $L_{low} = 10^{-6}$ to 10^{-5}. Values larger than 10^{-5} are displayed with the maximal box size. The relative interval width ϵ was chosen as $\epsilon = 4.1\%$.

The parameters characterizing the feedback operation are chosen as

$$\begin{aligned} t_{mem} &= 200 \\ \epsilon &= 0.041\,(= 4.1\%) \\ A_{amp} &= 100. \end{aligned} \tag{8}$$

To have some background against which the arising patterns can be easily discerned a threshold value L_{low} for the probability densities $\rho(t,j)$ is introduced. It both makes it possible to represent the patterns (consisting of sites with $\rho(t,j) \geq L_{low}$) in appropriate plots or diagrams and to define a physical lower limit for the operational properties of the system which will be discussed in detail below. We choose

$$L_{low} = 10^{-6}\,. \tag{9}$$

In Fig. (1), the evolution of $\rho(t,j) \geq L_{low}$ from time step $t = 800$ to $t = 900$ with the parameter sets of (5), (8), and (9) is displayed as density plot. The range of values of ρ between $L_{low} = 10^{-6}$ and 10^{-5} is indicated

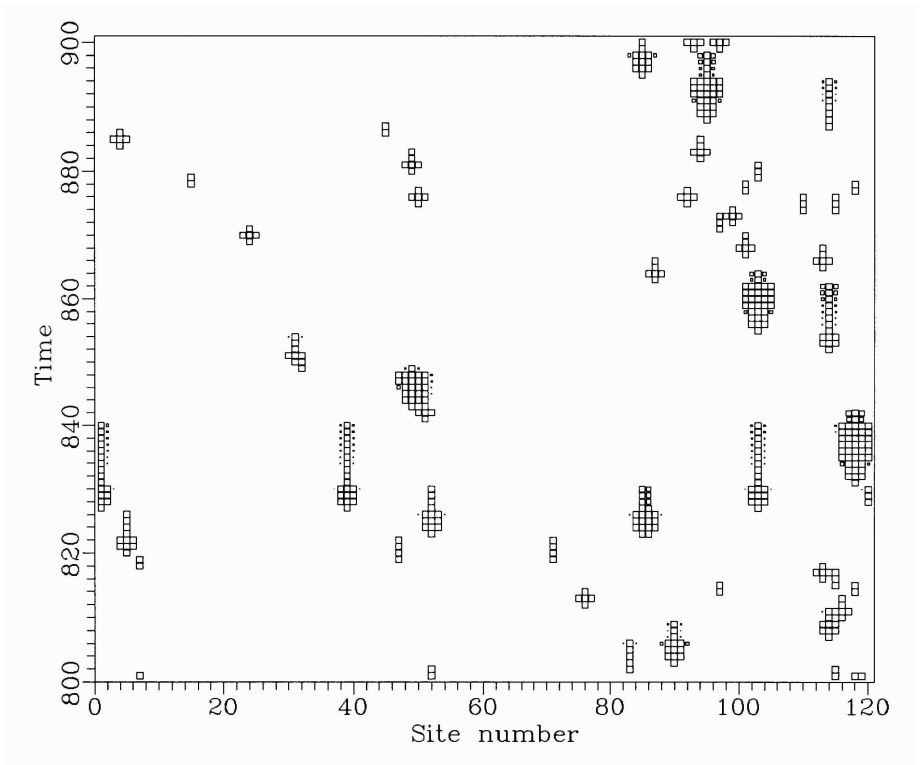

Figure 2: Density plot with the same conditions as in Fig. (1), but with $\epsilon = 25\%$. The fragmentation of the spatiotemporal patterns clearly has increased.

with different box sizes, whereas all values larger than 10^{-5} are displayed with the maximal box size. Due to the temporal feedback operation the continuous evolution of the QCA as studied in Ref. [10] gets disturbed after t_{mem}. The arising fragments, operationally defined by a group of spatially and temporally connected sites whose values are larger than the chosen limit L_{low}, are rapidly distributed all over the plane, irrespective of the patterns' locations due to the initial configuration. This feature can be understood in the following way: if a site fulfills the feedback condition, its value is strongly amplified relative to the neighbour's values. Thus it represents a nucleus for further evolution. After a certain time, another site will fulfill the time loop condition and will be enhanced, whereas the previous evolution will be damped after normalization. This behaviour continues until the damping process due to the appearance of new nuclei leads to an extinction of the evolving pattern which now remains as a fragment in the density plot.

This behaviour indicates a certain correlation between ϵ as measure for the probability of generating new nuclei on one hand, and the lifetimes τ of the fragments which depend on the frequency of the appearance of new nuclei on

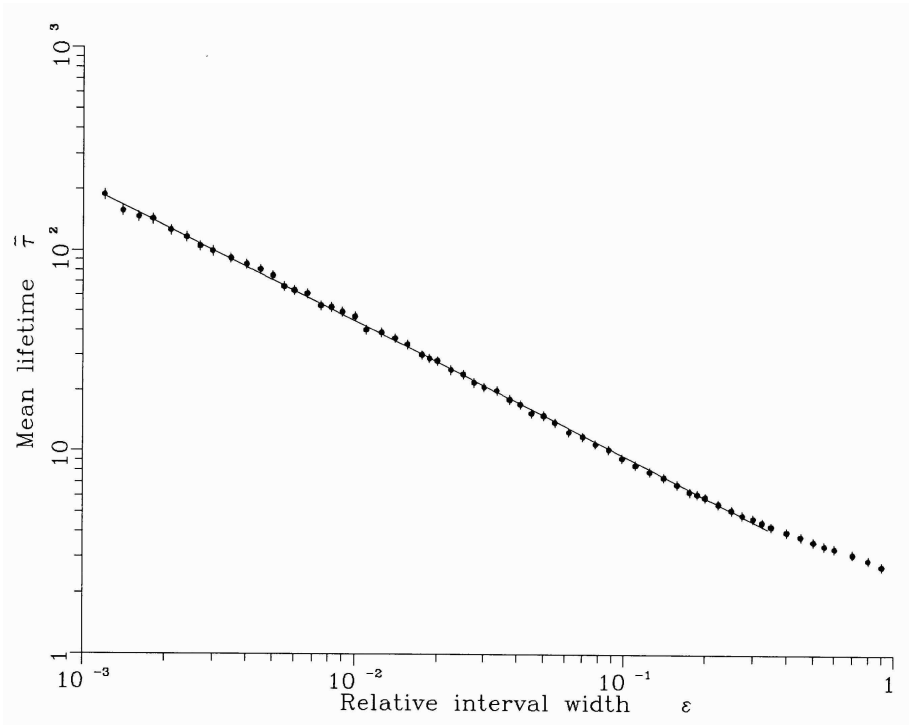

Figure 3: Log-log plot of the mean lifetimes $\tilde{\tau}$ of the fragments versus the relative interval width ϵ. Systems parameters are taken from Eqs. (5),(8), and (9). The data are fitted with a power-law function. Thus a "fractal evolution dimension" characterizing the pattern formation can be derived.

the other. This correlation can be seen from the comparison of Fig. (1) with Fig. (2), where ϵ has been enlarged up to $\epsilon = 25\%$. The fragmentation of the evolving patterns has clearly increased, and the mean lifetime of a single pattern has decreased. Therefore, a characterization of this new statistical property of the system by taking the mean lifetime of the patterns $\tilde{\tau} = \tilde{\tau}(\epsilon)$ is justified. Now the important role of a threshold value for ρ becomes clear: operationally, $\tilde{\tau}$, being a kind of "order parameter" of the system, has to be constrained by physical limits.

By varying ϵ between 0.12% and 90%, the plots were analyzed with regard to the mean lifetimes $\tilde{\tau}$ of the patterns. A "pattern recognition" program was written to count and analyze each bounded fragment up to $t = 5 \times 10^4$ and to calculate $\tilde{\tau}$ (simply as arithmetic mean) and its mean error σ. The latter includes also a systematical error, mainly due to ambiguities in choosing well defined fragments. With the help of parallel visual checks of the plots it was estimated as roughly 5% of $\tilde{\tau}$.

The result can be seen in Fig. (3), where the plotted data are shown in a log-

log diagram. As a surprising result, the data produce, at least up to $\epsilon \approx 35\%$, a linear function, indicating a kind of effective "fractal dimension" of the patterns independent of the relative interval width ϵ. The fit was performed with the power-law function

$$\tilde{\tau} = a \cdot \epsilon^b \tag{10}$$

where

$$a = 2.00 \pm 0.03, \quad b = -0.675 \pm 0.005 \tag{11}$$

with a χ^2 of 14.9 for 52 degrees of freedom.

We want to emphasize the difference in our use of b as opposed to the usual measure of a fractal dimension of an object. Usually, the fractal dimension exhibits an "object's" scale invariant features, whereby the process of its determination does not change the intrinsic properties of the "object". In our case, the scale invariance of the fragmentation of the evolving patterns is generated by the repeated application of different values of the relative interval width. We call this dynamical fragmentation process a "fractal evolution" of the system. The scale invariant property of the emerging order parameter of the system, characterized by the mean lifetimes of the patterns, will be denoted as "fractal evolution dimension" (D_E). In analogy to the usual algorithm [13, 14], one gets the "fractal evolution dimension" D_E as

$$D_E = 1 - b = 1.675 \quad \pm 0.005 \quad . \tag{12}$$

Note also that the fragmentation ceases (i.e. the lifetime of the pattern at the beginning goes to infinity) as ϵ goes to zero (i.e. when the precision of the comparison reaches a maximum). This behaviour is plausible, because the probability for the feedback condition getting fulfilled is very small for small values of ϵ, so that the evolution of the QCA remains nearly undisturbed.

The deviation of the data points in Fig. (3) from the linear function for $\epsilon \gtrsim 35\%$ can be understood at least qualitatively by looking at the shapes of the relative frequencies for the different lifetimes τ belonging to a specific ϵ. In Fig. (4), they are displayed for three different values of ϵ, i.e for $\epsilon = 0.9\%, 4.1\%$, and 25%, respectively. Note that with the default parameter values as introduced above no fragments of length $\tau = 1$ can occur: assuming the enhancement of some site at location j and time t, the value of $\rho(t, j)$ will be about 1.0 after normalization, whereas the other sites will be damped by a factor of about $\mathcal{N} \approx A_{amp}^2 = 10^4$. Even if, at the next time step, 10 different sites would fulfill the feedback condition and thus become enhanced, the normalization factor would be of the order $\mathcal{N} \approx 10 \times 10^4$. Therefore, $\rho(t+1, j)$ would indeed be reduced to about 10^{-5}, but it would still remain above the chosen threshold of $L_{low} = 10^{-6}$. Thus, a minimum length of 2 for each arising fragment is guaranteed.

The distributions are all asymmetric, showing poisson-like "tails" proportional to $e^{-\tau}$, but for large ϵ the cut-off at the lifetimes' value of $\tau = 2$ becomes effective. Thus, no fragments with $\tau < 2$ can contribute, and the mean value of those lifetimes will be shifted to a higher value.

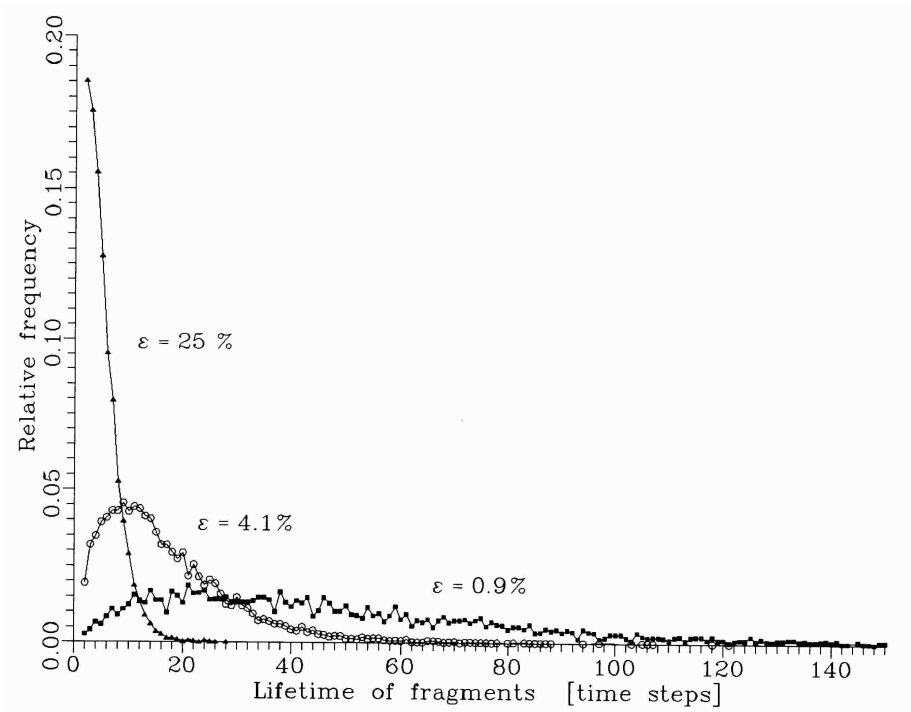

Figure 4: Distribution function of the patterns' lifetimes obtained for $t_{mem} = 200$ and for $\epsilon = 0.9\%$, $\epsilon = 4.1\%$, and $\epsilon = 25\%$, respectively. Characteristic asymmetric functions are observed.

We also report briefly on the variation of the systems parameters [15]. It turned out that fractal evolution is practically invariant under *i*) variation of the phase of the coupling parameter δ (cf. Eq. (5)), *ii*) the initial values of the state variables, and *iii*) the choice of other time intervals (than from t_{mem} to $t = 5 \times 10^4$) for the pattern analysis.

The variation of the remaining variables in (5), (8), and (9) in most cases also yields fractal evolution, but with shifted values of a and b in (11). Deviations from fractal evolution are observed in cases of "transient states" of the system according to specific values of the parameters. In all cases where such a deviation occurs also the shape of the distribution function for $\tilde{\tau}$ deviates from that described above.

Finally, even the rule (3) itself can be changed in an appropriate way without loosing the property of fractal evolution. For example, one can model a transition to a "semi-classical" system by restriction to real-valued parameters and couplings, i.e.

$$\Psi(t,j) = \frac{1}{\sqrt{\mathcal{N}(t)}}\{\Psi(t-1,j) + \delta[\Psi(t-1,j-1) + \Psi(t-1,j+1)]\} \qquad (13)$$

with Ψ, $\delta \in \mathcal{R}$. Also in this case a fractal evolution can be observed. This is opposed to the effects of the restriction to real values in the undisturbed case [10], where a "real-valued QCA" always leads to trivial final states.

3 Conclusions

An implementation of a specific temporal feedback operation in normalized dynamical systems on a lattice with a linear mapping function provides new and surprisingly rich evolutionary properties. Specifically, the temporal behaviour of QCA evolution with feedback loops selecting and amplifying particular regularities was investigated. We have found that these regularities are independent of the initial point configurations, of the phase of the coupling parameter, and of the choice of the time interval whithin which pattern analysis is performed.

Most importantly, we have found a strict scaling behaviour of the emerging spatiotemporal patterns: on a log-log scale, lifetimes $\tilde{\tau}$ of the patterns' fragments are a strictly linear function of the relative interval width ϵ fed back into the loop comparing the amplitudes at different evolution times. In other words, there exists a "fractal evolution dimension" D_E of the patterns whose value is independent of the particular choice of ϵ. As ϵ is the <u>relative</u> interval width, D_E is a quantity characterizing all the emerging patterns irrespective of the absolute values of the intervals in the temporal feedback loop. Above all, the observed features are not restricted to one specific model. It can be concluded that discrete, normalized feedback systems with linear mapping functions generally exhibit the property of fractal evolution [16].

Apart from being a "toy model" to study pattern generation in nonlinear systems, the observed features of our model are of particular interest for possible applications of QCA like modelling processes in the brain as discussed in Ref. [12]. As much of the encoding and decoding of neural signalling is a function of the "lifetimes" of neural firing, we have seen that our model is of interest because the system generating the characteristical "temporal patterns" does not have to operate with a "knife's edge" precision. On the contrary, our model gives an example of the unimportance of precision in some pattern recognition tasks: It just takes any two values for the average lifetimes $\tilde{\tau}$ at different relative interval widths ϵ to determine the "fractal evolution dimension" D_E typical for the feedback loop in the QCA, and thus to obtain a measure of $\tilde{\tau}$ under arbitrarily high precision ϵ (that is, within physical limits, of course). Such features may be relevant for real-time analog signal processing (as opposed to digital "all-or-nothing" processing with correspondingly high precision requirements) which allows for high effective noise levels and fault tolerances of neural computations [17].

References

[1] G. Grössing and A. Zeilinger, Complex Systems 2 (1988) 197, Complex Systems 2 (1988) 611, and Physica D 31 (1988) 70

[2] See, for example, H.G. Schuster, Deterministic Chaos, VCH, Weinheim 1989

[3] H.G. Schuster (Ed.), Nonlinear Dynamics and Neuronal Networks, VCH, Weinheim 1991

[4] J.L. McCauley, Z. Naturforsch. 42a (1987) 547

[5] G. Oppo and R. Kapral, Phys. Rev. A 33 (1986) 4219

[6] K. Kaneko, Phys. Rev. Lett. 65 (1990) 1391

[7] K. Kaneko, Prog. Theor. Phys. 72 (1984) 480, and Physica D 34 (1989) 1

[8] S. Wolfram, Rev. Mod. Phys. 55 (1983) 601, and Physica D 10 (1984) 1

[9] G. Grössing and A. Zeilinger, Physica D 50 (1991) 321

[10] S.Fussy, G. Grössing, H. Schwabl and A. Scrinzi, "Nonlocal Computation in Quantum Cellular Automata", Phys. Rev. A 48 (1993) 3470, and references therein

[11] QCA with additional feedback loops can be denoted as "higher order QCA" in analogy to perturbation theory as opposed to an "undisturbed", "zero order QCA".

[12] G. Grössing, Cognitive Systems 3 (1992) 289 and J. Biol. Syst. 1 (1993) 55

[13] B. B. Mandelbrot, The fractal geometry of nature (W. H. Freeman, San Francisco, 1982)

[14] H. Takayasu, Fractals in the physical sciences (Manchester Univ. Press, Manchester and New York, 1989)

[15] Details will be discussed in a forthcoming paper.

[16] For a similar power law in a classically chaotic system, see C. Grebogi, E. Ott, F. Romeiras and J.A. Yorke, Phys. Rev. A 36 (1987) 5365 and references therein. This system, however, cannot be characterized by fractal evolution because its time scale τ quantifies an observed post-crisis behaviour as, e.g., an average chaotic transient lifetime and not dynamically generated spatiotemporal patterns.

[17] See, for example, W. Bialek et al., Science 252 (28 June 1991) 1854